

Force modulation for enhanced nanoscale electrical sensing

This article has been downloaded from IOPscience. Please scroll down to see the full text article.

2011 Nanotechnology 22 355706

(<http://iopscience.iop.org/0957-4484/22/35/355706>)

View [the table of contents for this issue](#), or go to the [journal homepage](#) for more

Download details:

IP Address: 130.89.195.9

The article was downloaded on 19/09/2011 at 13:12

Please note that [terms and conditions apply](#).

Force modulation for enhanced nanoscale electrical sensing

W W Koelmans¹, A Sebastian², L Abelmann¹, M Despont² and H Pozidis²

¹ MESA⁺ Institute for Nanotechnology, University of Twente, PO Box 217, NL-7500 AE Enschede, The Netherlands

² IBM Research—Zurich, Säumerstrasse 4, CH-8803 Rüschlikon, Switzerland

E-mail: w.w.koelmans@alumnus.utwente.nl

Received 13 May 2011, in final form 12 July 2011

Published 8 August 2011

Online at stacks.iop.org/Nano/22/355706

Abstract

Scanning probe microscopy employing conductive probes is a powerful tool for the investigation and modification of electrical properties at the nanoscale. Application areas include semiconductor metrology, probe-based data storage and materials research. Conductive probes can also be used to emulate nanoscale electrical contacts. However, unreliable electrical contact and tip wear have severely hampered the widespread usage of conductive probes for these applications. In this paper we introduce a force modulation technique for enhanced nanoscale electrical sensing using conductive probes. This technique results in lower friction, reduced tip wear and enhanced electrical contact quality. Experimental results using phase-change material stacks and platinum silicide conductive probes clearly demonstrate the efficacy of the proposed technique. Furthermore, conductive-mode imaging experiments on specially prepared platinum/carbon samples are presented to demonstrate the widespread applicability of this technique.

(Some figures in this article are in colour only in the electronic version)

1. Introduction

Conductive scanning probes are powerful tools to investigate and manipulate electrical properties of surfaces and thin films at the nanoscale. Application areas include semiconductor metrology [1], probe-based data storage [2–6], investigation of nanoscale electrical transport in materials [7, 8] and nanolithography [9]. Conductive probes can also be used to emulate nanoscale electrical contacts such as those occurring in nano-electro-mechanical (NEM) switches for low power electronic applications [10, 11]. For the widespread applicability of conductive probes, however, several challenges need to be overcome. Major challenges are related to sustaining a high-quality electrical contact between the tip and sample while not losing spatial resolution over a prolonged tip lifetime. The fast degradation of the tip apex due to wear and high current densities pose significant challenges to conductive-mode scanning probe microscopy (SPM). The abrasion of the tip apex is accelerated by the significantly high normal load force on the tip required to obtain a good electrical contact with the sample.

There has been considerable effort to overcome these issues by carefully selecting the tip apex material. Coatings such as gold and platinum are reported [12]. These coatings increase the contact area between tip and sample and are often troubled by wear and delamination of the metal film [13]. More elaborate, and also more expensive, solutions such as doped diamond coatings and all-diamond tips harden the tip [1]. A different approach is to employ all-metal tips such that wear of the tip apex does not result in the loss of conduction, but it does result in a loss of resolution. Recently, silicidation of the tip apex after application of a platinum coating was shown [14], which led to superior wear resistance and higher admissible tip currents as compared to silicon tips. The wear of such a platinum silicide (PtSi) tip apex, however, is still too high for the requirements posed by industrial applications such as electrical-probe-based data storage and semiconductor metrology. PtSi tips have been shown to outperform many other types in terms of contact resistance, wear characteristics and the admissibility of high current densities [15]. The required load force for PtSi tips is typically between 40 and

300 nN [14]. Reducing the load force causes further increase in contact resistance [16] or a loss of tip–sample contact.

The value of the load force at which electrical contact is sufficiently well established depends on several factors. First, it depends on the tip and sample materials and their susceptibility to oxidation. Second, the values of the resistances under investigation determine the allowed tip–sample contact resistance. The contact resistance should be significantly lower than the relevant series resistances of the experiment. Third, the conditions in which the experiment takes place. An ambient environment allows oxidation of many materials, supplies contaminants to tip and sample surface, and adds a fluid layer [17]. In the search for suitable materials for NEM switches, significant increases in contact resistance are reported due to the buildup of contamination on the contact [18].

For a tip to establish contact with the sample, fluid contamination layers have to be pushed away and thin oxide layers need to be pierced. Even for a tip and sample made of an inert and highly conductive metal like gold, a minimum load force of 5 nN is reported for tunnelling to be established [19]. The presence of a native oxide layer on either tip or sample can increase the required load force to 20 μ N. All these factors result in an unreliable electrical contact and the need for a robust method to contact a sample surface arises. The conventional approach to accomplish a good contact is to increment the load force while scanning and in this manner abrading any layers prohibiting contact; however, this approach is detrimental to tip sharpness.

In this paper we present a complementary strategy, a normal force modulation technique, to increase the reliability of nanoscale electrical contact and to reduce tip wear in conductive-mode SPM. The essential idea behind the proposed force modulation technique is to modulate the normal load force while the tip is in contact with the sample [20]. This modulation is achieved by actuating the cantilever at specific mechanical resonant frequencies which correspond to the normal modes of vibration. Unlike the tapping mode where the tip traverses a wide range of the interaction potential, during the proposed force modulation technique the tip motion is assumed to be less than a nanometre and the tip is exploring only a fraction of the interaction potential. The idea is inspired by the successful demonstration of force modulation techniques for the reduction and elimination of wear in non-conducting SPM applications [21–23]. In this paper, we show that the modulation of the normal force not only reduces wear, it also effectively enhances the electrical contact between the tip and sample. This surprising result will be investigated in great detail using a variety of experiments.

A possible implementation of the proposed force modulation technique is illustrated in figure 1. Once the cantilever is brought into contact with the sample, a sinusoidal force is added on top of the load force that acts on the tip. This forcing is usually achieved by means of a dither piezo underneath the cantilever base. Alternative means of actuation such as electrostatic and magnetic can also be employed.

The experimental details are presented in section 2, followed by the experimental results in section 3. A discussion

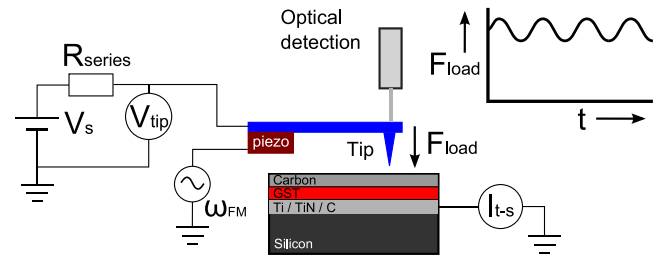


Figure 1. Schematic of the measurement set-up: a piezoelectric element underneath the cantilever base is employed to add a sinusoidal forcing on top of the load force. The sinusoidal forcing frequencies are chosen to be equal to specific mechanical resonant frequencies corresponding to the normal modes of vibration. Electrical circuitry is present to monitor the tip voltage (V_{tip}) and tip–sample current (I_{t-s}).

on the possible mechanism is presented in section 4, followed by the conclusions in section 5.

2. Experimental details

The experimental set-up consists of a home-built SPM with both optical deflection-sensing and conductive-mode operation capability. It is designed such that the micro-cantilevers can be mounted almost parallel to the sample (see figure 1). The sample is mounted on a commercial piezo scanning stage (Physical Instruments P517.3CL) with xyz -motion capability. The deflection of the cantilever is monitored using an optical beam deflection system equipped with a four-quadrant photodetector. A feedback loop is in place to adjust the sample height in order to ensure a constant load force. All experiments described are performed in ambient conditions at a relative humidity that ranges from 40 to 50%. During conductive-mode operation, a positive voltage is applied to the tip using voltage source V_s and the actual voltage over the tip (V_{tip}) is constantly measured. In regular operation the applied and measured voltages are almost identical because the value of series resistance ($R_{series} = 20 \text{ k}\Omega$) is small compared to the variable sample resistance, which is of the order of 1 $\text{M}\Omega$. A second electrical circuit is present to actuate the piezoelectric element, underneath the cantilever base, at the desired amplitude and frequency (ω_{FM}) for the force modulation.

We have made use of two types of cantilevers, both equipped with PtSi tips with a typical apex radius of 15 nm, see figure 2(b) for an example of a PtSi tip. Type 1 is a regular cantilever design with a fundamental resonant frequency of 67 kHz and a spring constant of 2.8 N m^{-1} . Type 2 is a cantilever with an anchor that fixes the cantilever to the chip base, see figure 2(a). Type 2 can be thought of as two cantilevers, the anchor and the protruding cantilever, in line and it will from now on be referred to as the dual cantilever. PtSi is chosen for the tip apex because it is a hard material, prevents oxide formation and forms an excellent nanoscale electrical contact [14, 15]. The PtSi was formed by depositing 10 nm of Pt on the tips using a liftoff process. Next, the tips are annealed at 700 $^{\circ}\text{C}$ for 5 min and then the remainder of the

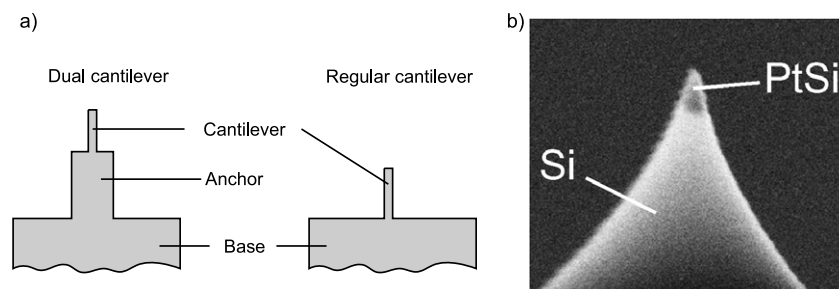


Figure 2. (a) Schematic drawings of the cantilevers used in this study and (b) a SEM image of a PtSi tip.

Pt is selectively etched. The full fabrication process of the PtSi tip and the dual cantilever is reported in [14]. The fundamental mode of the dual cantilever as a whole is around 70 kHz and of only the cantilever is around 100 kHz. The spring constant of the dual cantilever is 0.4 N m^{-1} , which is predominantly determined by the spring constant of the protruding cantilever.

Most of the experiments are performed on a phase-change layer stack deposited on a silicon substrate shown in figure 1. This sample is chosen for its relevance to probe-based data storage. One type of electrical probe storage employs phase-change materials such as germanium antimony telluride (GST) to store information by locally transforming its phase using a conductive probe. Phase-change materials are also very relevant for non-volatile memory applications [24]. The fabrication process is similar to that described in [25]. The stack we use consists of a bottom electrode of titanium (5 nm), titanium nitride (20 nm) and a nitrogen-doped carbon layer (100 nm), followed by the $\text{Ge}_8\text{Sb}_2\text{Te}_{11}$ active phase-change layer (12 nm) and finally a nitrogen-doped amorphous carbon top layer (6 nm).

3. Experimental results

3.1. Formation of electrical contact

In the first set of experiments we investigate the influence of force modulation on the formation of nanoscale electrical contacts. The objective of the experiments is to monitor the onset of electrical conduction. Tip-sample approach curves are performed whereby the PtSi tip is made to come into contact with the sample and then retract. The cantilever used is of type 1 and the sample is the phase-change stack.

The measurement is performed by ramping up the voltage on the z piezo of the scanning stage to bring the sample into contact with the tip. After the tip comes into contact with the surface the scanning stage is programmed to rise another 200 nm. Figure 3 shows the mean conductance of 100 sequentially obtained approach curves along with error bars indicating the standard error. After obtaining each approach curve a 5 nm sample move is performed in order to average out sample irregularity. The experiment has been performed three times with the same tip and sample; a reference measurement without any modulation, and two measurements with force modulation, one at contact resonance (267 kHz, 0.25 V amplitude) and one at 150 kHz, 0.5 V amplitude, in both cases for a tip voltage of 1.0 V. The resulting modulation

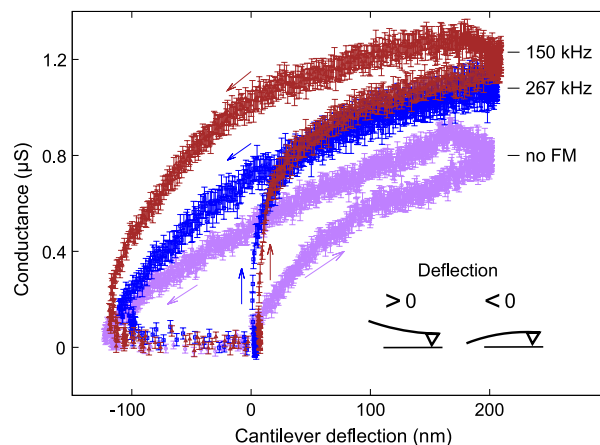


Figure 3. Conductance curves in normal mode (no FM) and with force modulation at 150 and at 267 kHz. Each curve is the mean of 100 consecutive experiments with standard error as error bar. With force modulation the electrical contact is significantly better at the moment the tip reaches the sample.

of the load force is estimated to be smaller than 10 nN, as explained in more detail in section 3.5. The data clearly show a much steeper evolution of the conductance at the moment the tip comes into contact with the sample surface when force modulation is applied. Moreover, with force modulation the conductance, after the first steep increase, is more constant with respect to the applied load. This means that the measured tip-sample current and the corresponding sample resistance are less dependent on the applied load.

All three conductance curves show a large amount of hysteresis at cantilever deflections smaller than zero due to the adhesive force between tip and sample. Remarkably, the curve without force modulation shows additional hysteresis at cantilever deflections greater than zero: the conductance in the forward regions is lower than the conductance in the backward region. The curve with force modulation at 150 kHz shows less hysteresis at cantilever deflections greater than zero. When using force modulation at 267 kHz the phenomenon has disappeared. This observation of increasing conductance while the load force is being reduced has been reported before [26, 27]. It is ascribed to a continued breakdown of an insulating fluid contaminant layer under the repulsive forces that continue to be exerted while the sample is retracting. The decrease, and even absence of the hysteresis at cantilever deflections greater than zero when force modulation is applied,

suggests that this mitigation of insulating surface layers is also achieved by a small dithering motion of the tip.

This observation has significant ramifications for nanoscale electrical contact studies, as in the case of NEM switches which are being investigated for ultra-low power applications. It suggests the potential of the force modulation technique to enhance the electrical contact quality between electrodes having a nanoscale contact area.

3.2. Conductive-mode imaging

One of the most important applications of conductive-mode SPM is to resistively map surfaces. This is essential for application areas such as semiconductor metrology and electrical probe storage. The influence of the force modulation technique in resistance mapping is investigated here in great detail.

We performed a series of imaging experiments in which the strength of the force modulation is varied. This is done by changing the amplitude of the oscillation voltage on the dither piezo. The experiments comprise 50 line scans (trace and retrace) each $2\ \mu\text{m}$ long and are performed on the phase-change stack with a set of cantilevers of type 1. After each scan the mean of the current is calculated, and friction data are extracted from the torsional motion of the cantilever, which is recorded during the scan. The experiment was repeated for several modulation frequencies; the fundamental resonance (67 kHz), the fundamental contact resonance (267 kHz) and two arbitrary frequencies in between. The data are obtained at a scan speed of $62.5\ \mu\text{m s}^{-1}$ and an average load force of 28 nN. The data at the 67 kHz modulation frequency are obtained at a scan speed of $10\ \mu\text{m s}^{-1}$ and at an increased average load force of 112 nN. During all measurements feedback on the vertical sample position is used to ensure a constant average load force. The tip voltage is set to 1 V. The mean values of current and friction are displayed in figures 4(a) and (b). The data are normalised with respect to the measurements at zero oscillation amplitude.

The shape of the curves differs with frequency, because the shape is governed by the tip motion. The tip motion, in turn, is determined by a frequency-dependent cantilever response. Moreover, there is an inevitable variation in the sharpness of the tips between the experiments, which influences the cantilever frequency response through the tip-sample interaction. Therefore, care has to be taken in comparing the curves at different modulation frequencies. It is, nonetheless, very clear that the trend of all the curves is similar. Specifically, for all frequencies of operation, starting at zero amplitude, a clear decrease in friction is observed. The lower friction is thought to be due to the periodic reduction in the normal force acting on the tip. This reduction reduces the barrier to lateral motion, allowing the tip to move without building up elastic strain. This analysis is in line with previous observations [22]. What is more surprising is the increase in average current with increasing forcing amplitude. The current is increased, in some cases, to more than three times the value at zero amplitude. An even further increase of the amplitude leads to a reduction in the average current. This reduction is

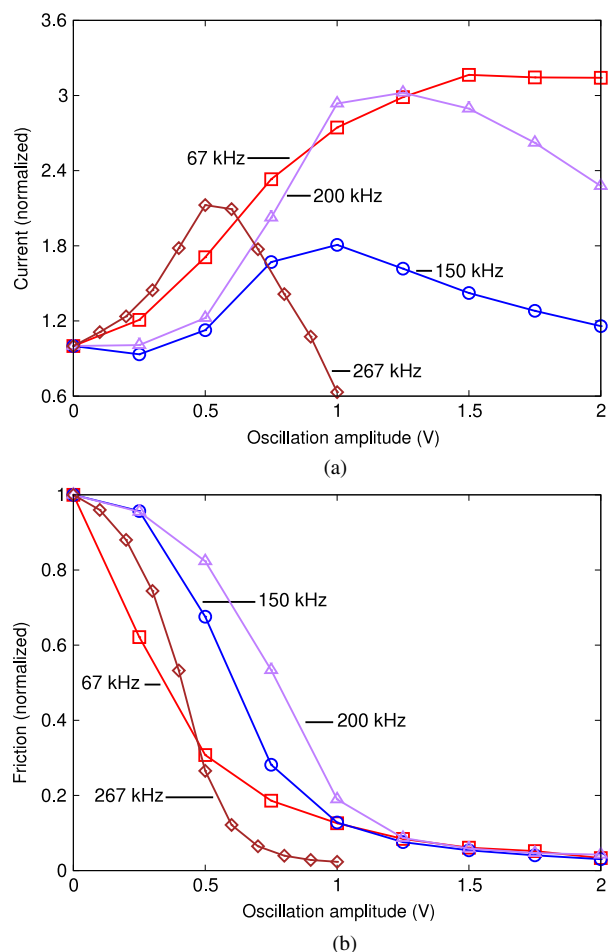


Figure 4. The mean of the tip-sample current (a) and the mean of the friction (b) during 50 line scans is plotted versus the amplitude of the piezo voltage. The frequency of the modulation is plotted for the fundamental resonance (67 kHz), the fundamental contact resonance (267 kHz) and two arbitrary frequencies in between.

attributed to too high a vertical tip motion, causing a partial loss of electrical contact. Therefore, at contact resonance a lower oscillation amplitude is used because the current peaks at an amplitude around 0.5 V. The decrease in contact resistance and friction also appears at other frequencies (150 and 200 kHz) than those associated with the normal mechanical resonances (67 and 267 kHz). Because the estimated tip motion that enhances the electrical contact is small, there is potential for the technique to work at a large range of frequencies that induce small tip motion normal to the sample surface.

3.3. Long-term imaging

To investigate whether the reduced friction indeed translates to reduced tip wear and whether the improved contact quality is sustained over extended periods of time, long-term imaging experiments are performed. In one of the experiments, the PtSi tip raster scans the phase-change stack for 1 m of tip travel. During the long-term wear experiment, continuous feedback using the z -scan axis is applied to ensure a constant load force. A total of 1250 raster scans of 0.8 mm of tip travel

is performed. Each scan yields topography and conduction images, of which every fifth is stored so that it can be checked for irregularities. After every raster scan, the adhesive force between tip and sample (F_{adh}) is measured from a tip-sample approach-and-retract curve. The adhesion force is a very good measure of the tip-sample contact area and thus an excellent means of *in situ* quantification of tip wear. Because the tip initially wears fast, a tip shape similar to that of a truncated cone is created. For this geometry the adhesion force is approximately proportional to the radius of the flat end a that is in contact with the sample [28]:

$$F_{\text{adh}} = ak_{\text{adh}} \quad (1)$$

where k_{adh} is a constant of proportionality. F_{adh} is thus a measure of tip wear. The wear experiments are performed at load forces of 10 and 20 nN, both with and without force modulation. A set of dual cantilevers is used and the force modulation is performed at the fundamental cantilever resonance frequency, i.e. approximately 100 kHz and at 0.5 V force modulation amplitude.

Figure 5(a) shows the results of the long-term experiments and clearly illustrates that, with force modulation, there is a substantial reduction in tip wear. The wear volume is estimated by overlaying the post-experiment and pre-experiment SEM images of the tips. For the 20 nN load experiments, these images are inserted in the graph. The contour of the fresh tip is indicated in the images after wear. A polynomial function is fitted to this contour to calculate the wear volume. At 20 nN load, force modulation reduces the wear by a factor of three (from 2.2×10^5 to 7.4×10^4 nm³). Moreover, wear curves with force modulation are evolving smoothly. These observations are consistent with the atom-by-atom wear model proposed in [28], in which the wear mechanism is thought to be a thermally activated bond-breaking process described by Arrhenius kinetics, where the barrier to remove an atom from the tip is lowered by the frictional shear stress acting on the tip. Hence, the reduced friction, which is caused by adding the force modulation, also translates to a reduction of tip wear. It is also important to note that, without force modulation, especially at the higher load force of 20 nN, the sharp decreases and subsequent increases in F_{adh} suggest that small parts of the tip break off. These breaking events temporarily sharpen the tip and lead to less predictable wear behaviour.

The mean current through the tip during each raster scan is plotted as a function of total tip travel in figure 5(b). The figure shows that, especially at 10 nN load force, the conducted current is considerably higher when force modulation is applied. In particular the average current over the full 1 m sliding distance is nine times higher for the 10 nN load force and 8% higher at 20 nN. From figure 5(b), it can also be seen that the relative variation in the mean current is appreciably smaller with force modulation. Note that for the experiment with 10 nN load force this is difficult to recognise because of the scale of the graph. Also note that the period of the regularly spaced peaks that are visible in two of the curves exactly match the interval between two consecutive visits of the tip to the same sample area. These experiments clearly illustrate the improved electrical contact quality over extended periods of time and across very long scan distances achieved by adopting force modulation.

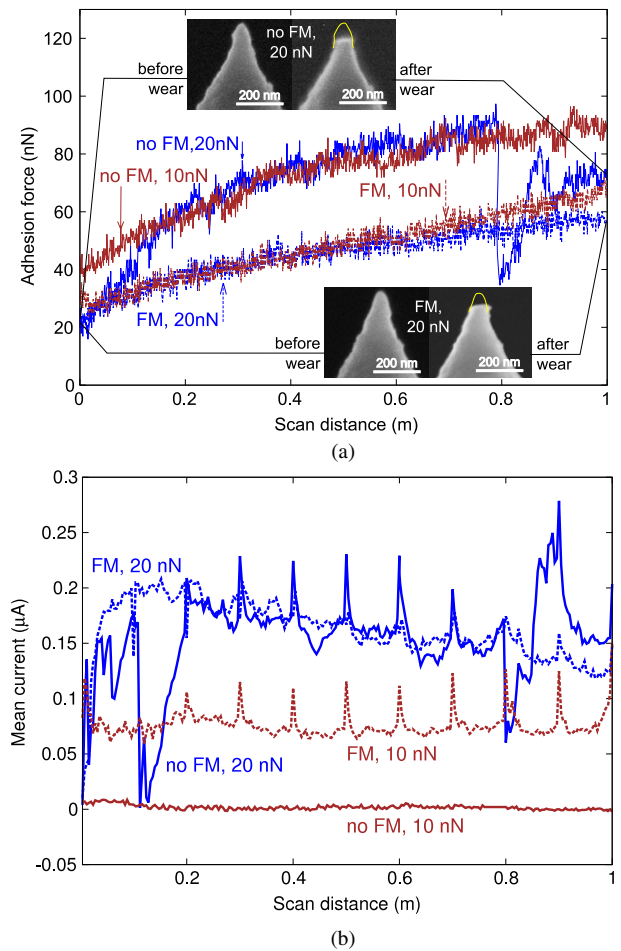


Figure 5. Tip wear and conduction during the long-term imaging experiments. The solid lines are without force modulation and the dotted lines with force modulation. (a) Force modulation gives lower wear rates. Insets: SEM images before and after the experiment. The contour of the fresh tip is shown in the images after wear. (b) The current data show a ninefold increased average current with force modulation at 10 nN load force.

3.4. Imaging of heterogeneous samples

Imaging experiments on heterogeneous samples are performed next to further illustrate the improved conduction with the force modulation technique and to assess its superior ability to differentiate between regions of variable electrical resistivity. Towards this end, a sample was prepared with small platinum pads on top of a phase-change material stack. The pads are approximately 300 nm in diameter and approximately 20 nm thick and were fabricated by evaporating platinum through a silicon nitride shadow mask. The presence of carbon, which is the capping layer on the phase-change stack, and platinum on the same sample surface enables us to assess the force modulation technique on two entirely different materials.

A dual cantilever with a fundamental cantilever resonance frequency of 99.3 kHz is used in the experiments. The dual cantilever has a seven times lower spring constant as compared to type 1 and thus provides better control over the load force. The images displayed in figure 6 show resistance maps at different load forces. The images on the left side show the

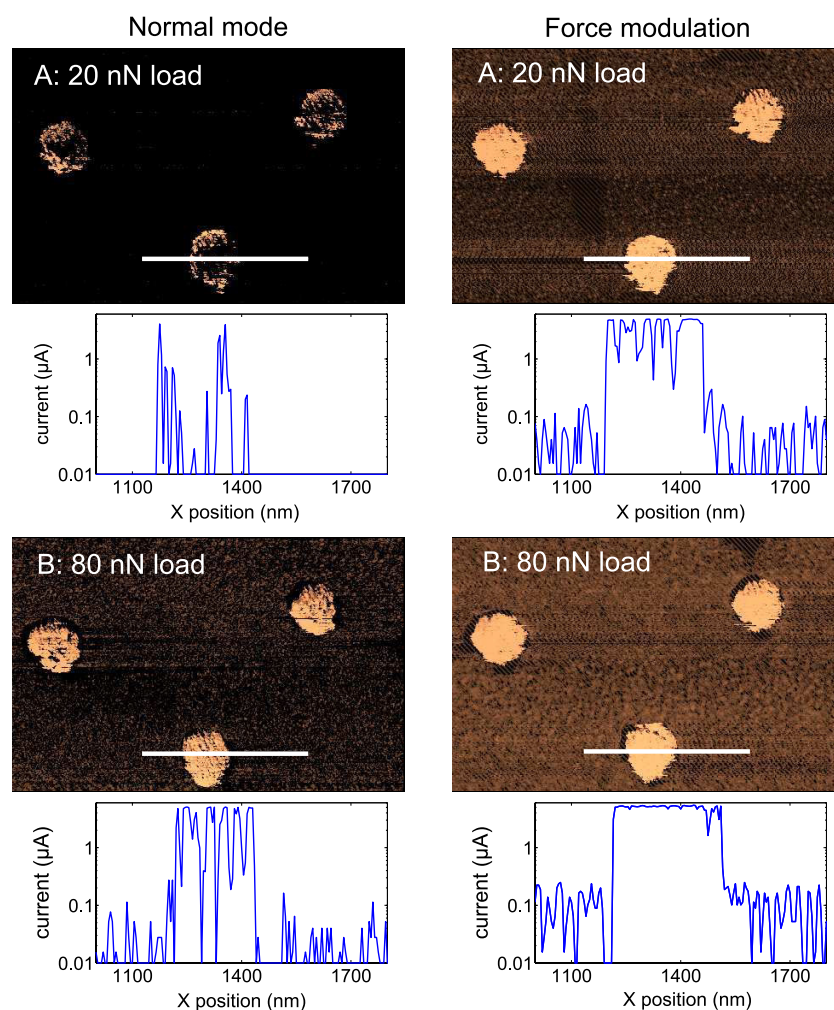


Figure 6. Resistance maps of platinum pads on a carbon background. The graphs show the current along a cross section indicated by the white lines in the images. The images and cross sections in normal mode show much more loss of contact than with force modulation. Note that all data are presented on a logarithmic scale.

result in conventional contact-mode conductive SPM and the images on the right side show the result when applying force modulation (99.3 kHz, 1.5 V amplitude). Again, a marked improvement in electrical contact between tip and sample is visible when force modulation is applied. Line profiles of the electrical current reveal that the difference in visibility of the pads in the resistance maps is caused by the capability of the tip to sustain the contact with the platinum surface. Although platinum is a material that is prone to contamination [18], the tip is able to pierce the contamination layer at exceptionally low load forces when force modulation is employed. At 80 nN load force with force modulation the contact with the surface is excellent. The small variation in current of approximately 100 nA, on the carbon layer is caused by the surface roughness of the sample.

For a series of load forces varying between 10 and 120 nN, the imaging of the sample is repeated and in figure 7 the ratio between the mean current over the entire surface with and without force modulation is plotted as a function of load force. It can be seen that at low load forces six times more current is conducted on average, whereas with increasing load force this ratio steadily drops towards unity. The marked data points A

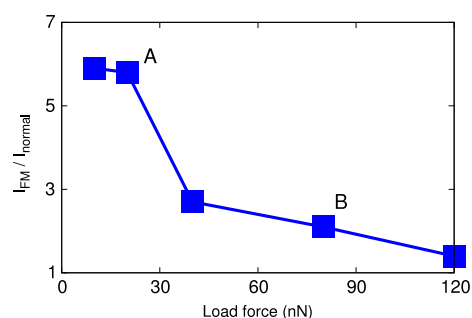


Figure 7. The mean current over the complete image is calculated and the ratio between the current with (I_{FM}) and without force modulation (I_{normal}) is plotted in the graph. The letters A and B refer to the measurements in figure 6.

and B correspond to the images in figure 6. It is evident from these measurements that lower load forces and the absence of force modulation lead to an increasing chance of contact loss.

In the above experiments, it is essential to confirm that the apparent reduction in contact resistance is not due to some fluctuating component of current created by the

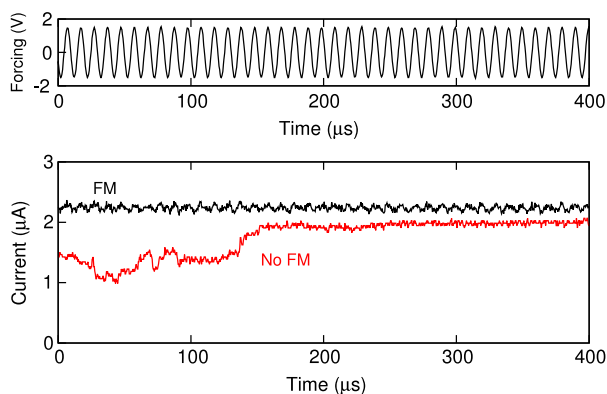


Figure 8. The tip–sample current measured at high bandwidth where the tip is on top of a platinum pad, with (top graph) the forcing signal and (bottom graph) the current, measured both with and without the force modulation (FM). A true reduction in contact resistance is seen, as well as a more stable current.

cantilever forcing and subsequent modulation of the tip–sample separation. In order to clarify this point, we performed a series of experiments where the signals are monitored at high bandwidth. Because our SPM is normally equipped with a low-pass anti-aliasing filter adjusted to the sample rate of 10–50 kS s^{−1}, the dynamics of the current signal at the timescale of one cycle of oscillation (approximately 10 μs) are not detected. The imaging experiments were repeated at 80 nN load force and a portion of the data were captured at a sample rate of 2.5 MS s^{−1}, while scanning at 10 μm s^{−1}. In figure 8 the forcing signal for the dither piezo together with the measured tip–sample current are shown. For comparison, the experiment is repeated without force modulation and superimposed onto the same graph. The data shown in figure 8 are taken from a low resistance area on a platinum pad. No clear, large peaks are observed in the current at the part of each oscillation where the load force is maximum. The DC part of the current is slightly higher in the presence of force modulation. This is a clear indication of a true reduction in the contact resistance. It is also seen that the reduction of the contact resistance is not the only cause of the increment in total conducted current; with force modulation the variation in conducted current is also less, in agreement with the data in figure 6.

3.5. Tip motion during imaging

It is beneficial to quantify the tip motion during the application of force modulation as it aids the basic understanding of this mode of operation. Unfortunately, such experimental measurements are hindered by the nature of the optical beam deflection system. This difficulty is because beam deflection monitors the angle of the cantilever rather than the vertical position of the tip. Off-contact, in fundamental resonance mode, there is a direct relation between the position of the tip and the angle of the cantilever; however, in-contact, when exciting the base of the cantilever, the cantilever will undergo additional bending because the applied moment is counteracted by the normal sample force. The applied moment results in a

rotation of the tip on the sample and thus causes an increased bending of the cantilever beam. Consequently, the measured deflection of the optical beam, approximately 6 nm peak-to-peak motion, overestimates the vertical motion of the tip. In order to obtain a first-order estimate of the true vertical tip motion we have employed a mechanical lumped element model with piecewise linear cantilever–sample interaction force which was presented in [29]. The model was adjusted to fit our experimental conditions using the dual cantilever. Based on calculations with this model, we estimate the tip oscillation amplitude to be approximately 0.4 nm for 1 V force modulation amplitude at 100 kHz. Here we use a cantilever stiffness of 0.4 N m^{−1} and assume a contact stiffness of 20 N m^{−1}. The resulting force modulation therefore has a peak-to-peak value of 9 nN.

4. Discussion

We have carried out a series of experiments which clearly demonstrate the ability of the force modulation technique to enhance the contact quality while forming a nanoscale electrical contact. This enhancement comes in addition to significantly lowered friction and reduced tip wear achieved by force modulation. It is hypothesised that the reduction in the contact resistance observed with the force modulation is due to the mitigation of any insulating barrier that is unavoidably present in ambient conditions. The periodic increment in load force causes the tip to reach the conductive sample surface despite contaminants; however, no large peaks in conduction during each oscillation period were found. The absence of such peaks indicates that the tip is consistently making good contact with the sample and the dithering motion of the tip aids in establishing and maintaining this contact. We speculate that the dithering motion causes a breakdown of the layer of contaminants covering the sample surface by expulsion or penetration of the insulating material. When the load force is reduced at every cycle of oscillation, this layer is not restored and the improved conductance is retained. This explanation is in agreement with previous work [26, 27, 30], in which the authors suggest a continuous expulsion or penetration of material during an approach–retract curve, even during the initial part of retraction of the tip. This increase in conductance is less apparent when force modulation is used and even disappears at certain modulation frequencies. This absence indicates that force modulation has a similar effect as many consecutive approach–retract curves, performed at high speed. If this speed is high enough, compared to the speed of scanning, the increase in conduction is effectively instantaneous. If the tip motion is too high, the resulting reduced tip–sample interaction leads to an increasing contact resistance. This increasing resistance agrees with the observation in figure 4(a) that too high an amplitude reduces the conductance. The relation between the frequency of modulation and tip amplitude is, however, not straightforward.

The hypothesised mitigation of the insulating barrier does not have a detrimental influence on tip wear, as was confirmed by the long-term imaging experiments. We believe that the reason the tip does not wear much due to the mitigation is that

the elastic modulus and hardness of the tip are much larger than any insulating barrier. Note that it has been reported in [6] that a water layer on the surface can act as a viscoelastic layer that reduces the stress acting on atomic bonds that take part in the wear process.

A possible additional contribution to tip wear is an increased tip temperature due to Joule heating, caused by the current that flows through the tip. The currents that are used in this paper are usually around 1 μA and do not exceed 3 μA . These currents will not result in a significant increase in the tip temperature. Moreover, the hottest region is usually a few nanometres into the sample due to the excellent heat conductivity of PtSi and Si. However, when higher currents flow through the tip, Joule heating could become an issue which potentially accelerates the tip wear process.

To summarise, the normal force modulation technique has been shown to improve the electrical contact quality in addition to reducing friction and wear at multiple frequencies. We see no reason to assume that other frequencies, in between the fundamental free resonance and the contact resonance frequencies, do not lead to similar results. Also, a range of amplitudes is available for which force modulation positively affects friction and conduction.

5. Conclusion

A novel force modulation technique is presented for conductive-mode SPM, whereby the tip-sample normal load force is modulated at specific frequencies during electrical sensing. These frequencies correspond to mechanical resonances associated with the normal modes of vibration. Using a mechanical lumped element model the resulting tip motion is estimated to be less than a nanometre. Experimental results using PtSi conductive probes and phase-change material stacks clearly demonstrate the efficacy of this technique. The force modulation technique has a significant influence on the formation of nanoscale electrical contacts. In conventional contact-mode operation the conductance increases with applied load force, whereas with force modulation the formation of a high-conductance electrical contact is almost instantaneous, as shown from conductive-mode approach curve experiments. Conductive-mode imaging experiments clearly illustrate the increased electrical contact quality in addition to reduced friction and wear. Imaging experiments spanning a metre of tip travel demonstrate the long-term reliability of this technique. Due to force modulation a wear reduction of more than three times for PtSi tips is demonstrated and the experiments show no signs of breaking of the tip apex. During long-term imaging a ninefold increase of the average current was measured. The mechanism behind the wear reduction is shown to be a decrease in friction between tip and sample due to the periodic reduction in load force, which prevents the buildup of lateral forces on the tip. The increased electrical contact quality is hypothesised to be due to the improved piercing of a layer of contaminants covering the sample surface. The periodic increase of the load force aids the normal forces to push the tip into the repulsive regime, where good electrical contact quality can be maintained. Imaging experiments were

also performed on specially prepared heterogeneous samples consisting of evaporated platinum marks on an amorphous carbon background. The force modulation scheme proves to be especially beneficial at lower load forces. An almost sixfold increase of mean conducted current was measured at a load force of 10 nN. Low load forces are of great interest because they exert a much lower wear rate. Force modulation is beneficial over a wide operation range, can be performed at multiple frequencies and is tunable to a sweet spot with low friction and enhanced electrical contact. This technique could have a significant impact on nanoscale electrical sensing using conductive-mode SPM.

Acknowledgments

The authors gratefully acknowledge Andrew Pauza for the GST samples, Laurent Dellmann for the platinum samples, Ute Drechsler and Walter Haerberle for experimental support, and Harish Bhaskaran and Niels Tas for helpful discussion. The authors gratefully acknowledge NanoWorld AG for the supply of some of the platinum silicide cantilevers used in this work. This work is supported by the European Research Council within the FP6 project 'Probe-based Terabit Memory'.

References

- [1] Oliver R A 2008 *Rep. Prog. Phys.* **71** 076501
- [2] Wright C D, Armand M and Aziz M M 2006 *IEEE Trans. Nanotechnol.* **5** 50–61
- [3] Tanaka K, Kurihashi Y, Uda T, Daimon Y, Odagawa N, Hirose R, Hiranaga Y and Cho Y 2008 *Japan. J. Appl. Phys.* **47** 3311–25
- [4] Jo A, Joo W, Jin W H, Nam H and Kim J 2009 *Nature Nanotechnol.* **4** 727–31
- [5] Wuttig M and Yamada N 2007 *Nature Mater.* **6** 824–32
- [6] Tayebi N, Zhang Y, Chen R J, Tran Q, Chen R, Nishi Y, Ma Q and Rao V 2010 *ACS Nano* **4** 5713–20
- [7] Kügeler C, Nauenheim C, Meier M, Rüdiger A and Waser R 2008 Fast resistance switching of TiO₂ and MSQ thin films for non-volatile memory applications (RRAM) *NVMTS: 9th Annual Non-Volatile Memory Tech. Symp. (Pacific Grove, CA)* pp 1–6
- [8] Sebastian A, Pauza A, Rossel C, Shelby R M, Rodriguez A F, Pozidis H and Eleftheriou E 2011 *New J. Phys.* **13** 013020
- [9] Vasko S E, Kapetanović A, Talla V, Brasino M D, Zhu Z, Schöll A, Torrey J D and Rolandi M 2011 *Nano Lett.* **11** 2386–9
- [10] Lee T H, Bhunia S and Mehregany M 2010 *Science* **329** 1316–8
- [11] Chen F, Kam H, Markovic D, Liu T J K, Stojanovic V and Alon E 2008 Integrated circuit design with NEM relays *ICCAD: Int. Conf. on Computer-Aided Design (San Jose, CA)* pp 750–7
- [12] John N S and Kulkarni G U 2005 *J. Nanosci. Nanotechnol.* **5** 587–91
- [13] Bussmann E and Williams C C 2004 *Rev. Sci. Instrum.* **75** 422–5
- [14] Bhaskaran H, Sebastian A, Drechsler U and Despont M 2009 *Nanotechnology* **20** 105701
- [15] Bhaskaran H, Sebastian A and Despont M 2009 *IEEE Trans. Nanotechnol.* **8** 128–31
- [16] Brezna W and Smoliner J 2008 *J. Appl. Phys.* **104** 044309
- [17] Moreland J, Russek S E and Hopkins P F 1997 *IEEE Trans. Magn.* **33** 4068–70
- [18] Chen L, Lee H, Guo Z J, McGruer N E, Gilbert K W, Mall S, Leedy K D and Adams G G 2007 *J. Appl. Phys.* **102** 074910

- [19] Meepagala S C, Real F and Reyes C B 1991 *J. Vac. Sci. Technol. B* **9** 1340–2
- [20] Koelmans W W, Sebastian A, Despont M and Pozidis H 2010 Force modulation for improved conductive-mode atomic force microscopy *IEEE NANO 2010: 10th IEEE Conf. on Nanotechnology (Seoul)* pp 875–8
- [21] Radmacher M, Tillmann R W, Fritz M and Gaub H E 1992 *Science* **257** 1900–5
- [22] Lantz M A, Wiesmann D and Gotsmann B 2009 *Nature Nanotechnol.* **4** 586–91
- [23] Knoll A, Rothuizen H, Gotsmann B and Duerig U 2010 *Nanotechnology* **21** 185701
- [24] Wetnic W and Wuttig M 2008 *Mater. Today* **11** 20–7
- [25] Bhaskaran H, Sebastian A, Pauza A, Pozidis H and Despont M 2009 *Rev. Sci. Instrum.* **80** 083701
- [26] Mate C M, Erlandsson R, McClelland G M and Chiang S 1989 *Surf. Sci.* **208** 473–86
- [27] Morita S, Ishizaka T, Sugawara Y, Okada T, Mishima S, Imai S and Mikoshiba N 1989 *Japan. J. Appl. Phys.* 1 **28** 1634–6
- [28] Gotsmann B and Lantz M A 2008 *Phys. Rev. Lett.* **101** 125501
- [29] Sebastian A, Salapaka M V, Chen D J and Cleveland J P 2001 *J. Appl. Phys.* **89** 6473–80
- [30] Mamin H J, Ganz E, Abraham D W, Thomson R E and Clarke J 1986 *Phys. Rev. B* **34** 9015–8